Arabian Journal of Geosciences (2021) 14: 2390
https://doi.org/10.1007/s12517-021-08674-z

ORIGINAL PAPER

Machine learning techniques for recycled aggregate concrete strength prediction and its characteristics between the hardened features of concrete

Shamili Syed Rizvon[1] · **Karthikeyan Jayakumar**[1]

Received: 19 July 2021 / Accepted: 20 October 2021 / Published online: 10 November 2021

Abstract

This study aims to arrive at models to correlate the mechanical properties of recycled aggregate concrete (RAC). An experiment was performed on the recycled coarse aggregate (RCA) ratio of 0%, 25%, 50%, and 100% with 400kg/m^3 of cement content, varying water-to-cement ratio (w/c) 0.3, 0.4, 0.48, and super plasticizer (SP) dosage to produce 15 different mixes were investigated. Furthermore, the compressive strength (both cube f_{cu} and cylinder f_{cyl}), modulus of elasticity (E_c), split tensile strength (f_{ct}), and flexural strength (f_{cr}) were tested and investigated. In view of the results, new models representing the impact of RCA were created. The results showed that in terms of replacement ratio, at 56d, the mix with 25% of RCA with water-to-cement ratio (w/c) 0.3 and super plasticizer (SP) 1.5%, recorded maximum strength of 59.86MPa, 4.81MPa, and 5.416MPa under cube compressive strength, split tensile, and flexural strength respectively. The proposed models can effectively predict the E_c, f_{ct}, f_{cr}, f_{cyl}, and f_{cu} of RAC. Scanning electron microscope (SEM) was conducted to scrutinize the microstructure of selected mixes which shows comparatively low voids, micro-cracks, and pores. Also, machine learning techniques like multi-linear regression (MLR) and extreme gradient boosting (XGB) algorithms were utilized for the compressive strength prediction of concrete (CSC). Results indicated that XGB for cylinder compressive strength was found to be 2.7% greater than cube compressive strength and MLR for cylinder compressive strength was found to be 1.5% greater than cube compressive strength

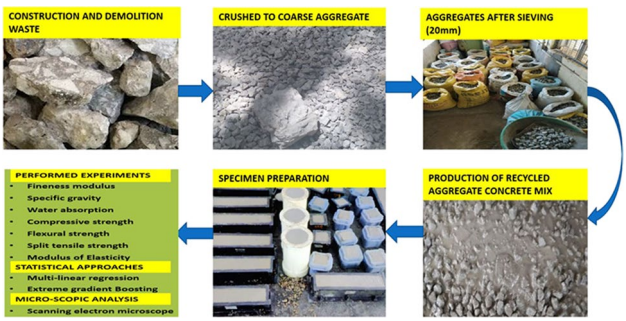

.

Keywords Recycled aggregate concrete · Recycled coarse aggregate · Compressive strength · Multi-linear regression · Gradient boosting

Communicated by Amjad Kallel

✉ Shamili Syed Rizvon
shamili.sr@gmail.com

[1] Department of Civil Engineering, National Institute of Technology, Tiruchirappalli 620015, India

Abbreviations

RAC	Recycled aggregate concrete
RCA	Recycled coarse aggregate
W/C	Water-to-cement ratio
WC	Water content
SP	Super plasticizer

NAC	Natural aggregate concrete
NCA	Natural coarse aggregate
F_{cu}	Cube compressive strength
F_{cyl}	Cylinder compressive strength
F_{ct}	Split tensile strength
F_{cr}	Flexural strength
MOE	Modulus of elasticity
GA	Genetic algorithm
ANFIS	Adaptive neuro fuzzy interference system
MLR	Multi-linear regression
XGB	Extreme gradient boost
SEM	Scanning electron microscope
CSC	Compressive strength of concrete
FA	Fine aggregate
CDW	Construction and demolition waste

Introduction

Concrete is the most broadly utilized structure material in the development industry. These days, it is assessed that the creation of cement may accomplish over of 10 billion tons each year on the earth. Despite the vast production and use of concrete around the world, there has been much speculation that it could be a significant contribution to greenhouse gas emissions. Furthermore, the combustion of natural resources and fossil fuels emits enormous amounts of gases during the production of cement (Qian et al. 2018). A total of 4 billion tonnes of Portland cement are manufactured each year, with one tonne of cement producing one tonne of CO_2 (Akbar and Liew 2020). A procedure of substituting the cement material with an alternative binder is of major scientific interest to address the aforementioned difficulty. Given the current state of the climate and the phenomenon of global warming, a green revolution in the construction and other industries is urgently needed - in other words, enterprises must embrace and develop environmentally friendly materials. Bagasse ash, rice husk ash, and other industrial and agricultural waste products are some of the examples of supplementary cementitious materials utilized in the cement industry. However, silica fume, fly ash, and ground granulated blast furnace slag are extensively adopted and employed in the building industry. With this awareness, the concrete industry has fortunately discovered various sustainable and environmentally friendly concrete alternatives such as plastic waste, electronic waste, construction, and demolition waste. The significant use of construction and demolition wastes (CDW) likely could be the sensible and planned approach to manage those issues as signified (Marinković et al. 2010). Zhang et al. (2019); Angulo et al. (2009); Rao et al. (2011) have inferred the issues from CDW are expanding up due to the speeding up of urbanization in the non-industrial countries, particularly in China, Brazil, and India. Even though the reusing for CDW has been led for over 50 years, at this point it simply covers the utilization of coarse aggregates and their utilization is limited because of the low strength and flexible modulus, low workability, high water penetration, high shrinkage, and creep of RAC has revealed (Poon and Chan 2007; Soutsos et al. 2011). Because of the low density and high porosity of RCA, RAC likely could be essentially more porous than natural aggregate concrete (NAC) which was showed (Evangelista and de Brito 2010; Zaharieva et al. 2003) and the compressive strength of RAC could presumably be considerably less than that of NAC which was exemplified (Sim and Park 2011; Corinaldesi and Moriconi 2009; Lee 2009). Better results of RAC mixes were obtained till 40% substitution of RCA was inferred (Ahmed 2013; Daniel Matias et al. 2014; Sivakumar 2014; Prasad et al. 2021) and later on Lee (2009); Corinaldesi (2010) revealed that most extreme substitution of natural coarse aggregate (NCA) by RCA was as yet confined to under 50%. Belén et al. (2011) exhibited that the primary properties of RAC began to concentrate after the 2000s to apply RAC into real design. It is shown that an ultimate strain of RAC diminished with the expansion of the substitution by RCA from the aftereffects of the axial compression test, although the substitution of 50% NCA by RCA showed a slight impact on a deflection from the shear test consequences of RAC beams was signified (González-Fonteboa and Martínez-Abella 2007). The properties of RCA influenced by the porous ITZ which may likely be the most fragile point in RAC because the strength of adhered mortar in RCA typically was much lower than that in NCA was illustrated (Etxeberria et al. 2007; Poon et al.(2004; Rawaz-Kurda and Silvestre 2020). A similar report surmised that using different extents of RCA and W/C with dissimilar moisture conditions, the strength was discovered to be around 10% to 25% lesser contrasted with NAC, and in this way, the full substitution of RCA ordinarily decrease the substantial strength and thusly ought to be kept away from. This impact has been generally contemplated as demonstrated (Ajdukiewiez and Kliszczewicz 2002; Hansen and Narud 1983; Tsung et al. 2006; Ryu 2002). Thusly, bits of exploration have been directed to anticipate the substantial compressive strength. The development business is believed to be overwhelmed with asset planning, hazard the executives, and arrangement challenges which consistently end in style absconds, project conveyance delays, value invades, and composed understanding questions. These difficulties have prompted examination inside the use of cutting edge AI calculations like profound figuring out how to help with the demonstrative and prescriptive investigation of causes and preventive measures. As such to enhance the exploration and to minimize the expense and time required for testing, the models reliant upon test information anticipating the CSC with a palatable extent of blemish may be upheld. As

a result, research is needed to develop a robust model that employs machine learning techniques and can properly estimate the compressive strength of concrete. Specialists in the development business have made a few astounding endeavors to stay aware of the speed of applying profound learning denoted (Taofeek et al. 2020). According to Ahmad et al. (2021), machine learning techniques should also be utilized to forecast the impacts of the environment on concrete properties. Machine learning algorithms, as outlined in the paper, can reduce time in the lab and predict the outcome by collecting a large amount of data. Because they anticipate the values of multiple variables, machine learning algorithms are more effective than simple correlation models. As a result, research is needed to develop a precise prediction that employs machine learning techniques that can accurately predict CSC. Vivian et al. (2008) indicated fake neural networks. Regression investigation are a portion of the procedures that were executed to foresee the compressive strength of RAC. The associations among destroyed substantial properties and strength of their RAC were set up utilizing relapse investigation. Additionally, other information driven-models like linear regression and model trees were utilized to show CSC as expressed (Deepa et al. 2010). During the continuous years, a phenomenal thought by the specialists of material science has been expanded unequivocally for the 28-days CSC on account of material mechanical property as signified (Neter et al. 1996; Hong-Guang and Ji-Zong 2000; Oztas et al. 2006; Bilim et al. 2009; Ramezanianpour et al. 2004; Purushothaman et al. 2015; Özcan et al. 2009) while, for the check of novel soft computing systems it is used as a fundamental model as explained (Yilmaz and Yuksek 2009). As a dynamic method, in regression analysis, the correlation between a response variable which is the dependent variable, and one or more independent variables are utilized for assessment as expressed (Waszczyszyn and Słoń ski 2010). XGB is an extreme gradient boosting algorithm which is a valuable device to predict the compressive strength of concrete and in helpful underlying structure applications with more prominent speed and accuracy in contrast with other artificial models as showed (Yu Li et al. 2019; Tamayo et al., 2016; Duan et al. 2020). Also, XGB for structural health monitoring and in anticipating the cross-tension strength of self-piercing riveted joints, showed high coefficient of regression and low RMSE value which achieves better exactness as revealed (Donga et al. 2020; Lin et al. 2020). Bagging as an ensemble strategy for high-performance concrete mix slump flow has been compared in the literature (Aydogmus et al. 2015). In comparison to single techniques, ensemble models with bagging were found to be superior. For predicting concrete corrosion in sewers, Zounemat-Kermani et al. (2020) represents the performance of five soft, computer base learners. The author tested both tree-based and network-based learners, and found that ensemble learners outperform them with an R^2 of 0.872. These ensemble methods produce a more powerful effect while ensuring that the overall models work well. Ahmad et al. (2021) infers that, when compared to a decision tree used alone or with gene expression programming, a decision tree with ensemble modelling provides a more stable result with $R^2 = 0.911$. Also, statistical tests demonstrate that the decision tree with ensemble improves MAE, MSE, and RMSE between the target and outcome response by 25%, 121%, and 49%, respectively.

Considering the foregoing, it may appear that tree based ensemble learning models have more favorable characteristics and produce better results than individual learning models.

Research significance

Many attempts were made on the prediction of concrete compressive strength using ANN, ANFIS, GA, and MLR. But possibilities on the prediction of recycled concrete compressive strength using gradient boosting algorithm were not attempted. Moreover, the difference in the statistical approach using gradient boosting was not available in the literature.

The goal of this study is to arrive at many relationship models to correlate the hardened properties of RAC mixes. Still, only a few researchers have attempted to develop a correlation model on the RAC, but less focused on comparing the statistical models using the machine learning techniques such as multi linear regression, and extreme gradient boosting. These are the novel research gap distinguished in the writing. Wherefore, this study focuses on evaluating the hardened mechanical properties of full and partial replacement of RAC on 400kg/m^3 of cement content with varying w/c, and SP dosage. With the obtained results, correlations between the various hardened properties were proposed. Also, by using the machine learning techniques, MLR and boosting algorithms like XGB were performed to predict the compressive strength of recycled aggregate concrete. The outcome of this present study contributes new knowledge to the existing literature in the area of identified research gaps.

Materials

Binders

At standard temperature, Rapid Hardening Portland Cement, portrayed with higher fineness, hydrates more rapidly than any other sort of cement. Wherefore, at the initial phase of hydration for instance 1, 3, and 7 days at determined w/c, the concrete containing Rapid Hardening Portland Cement

concrete has lower porosity and higher quality. In comparison to Rapid Hardening Portland Cement, the rate of hydration and quality improvement at Ordinary Portland Cement with Portland-slag and Pozzolana Portland cement are delayed up to 28 days as expressed (Newman and Choo 2003; Jankovic et al., 2011). In this research, ASTM type IP (Portland pozzolana cement with 40% natural pozzolana) with cement content of 400Kg/m^3 has been used. The cement sample showed a compressive strength of 56Mpa at 28 days, which satisfied the grade 53 strength criteria as specified in IS 269:2015. This cement content was chosen since it was found to be effective in terms of strength (Eskandari-Naddaf and Azimi-Pour 2016; Almusawi et al. 2020) and safe against all the exposure conditions as specified in IS 456:2000. The properties of this binder were tested as detailed in IS: 4031 2005 and tabulated in Table 1.

Fine aggregates

Jankovic et al. (2011) expressed, when compared to the binder and ITZ in concrete, the aggregate particle is considered to be stronger. According to IS 383:2016, river sand conforming to zone II was utilized in this research with a particle size less than 4.75mm. The material property of the fine aggregate and gradation curve has been shown in Table 1 and Fig. 1 respectively.

Recycled coarse aggregate

RCA samples were collected from a demolished building in Tiruchirappalli, Tamil Nadu. The RCA samples were manually crushed, then crushed again using a lab model jaw crusher and sieved. The crushed stone having a particle size of 20 mm, has been utilized as RCA. The physical attributes of the aggregate were tested as per IS 2386: 2002. Material property and particle size distribution of NCA, and RCA has been shown in Table 1 and Fig. 1 respectively.

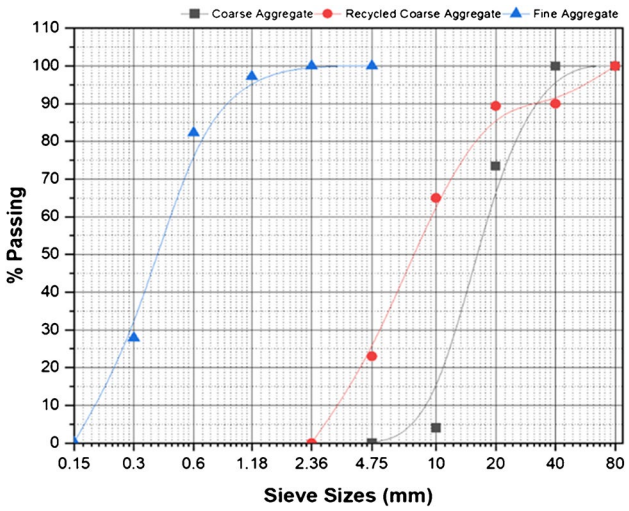

Fig. 1 Sieve analysis

Super plasticizer

Under BS: 5075–3, the SP utilized in this research was Conplast SP-430 and relying upon the dosage measurements utilized and meets the rules in IS 9103:1999. Table 1 indicates the properties of the materials used.

Modeling techniques

In model prediction, to gain from the assortment of training patterns a stage contains a "training" process that helps the model. Multi-linear regression and gradient boosting are two distinct models utilized in this study for the CS prediction of RAC. The executions of these models depend on the coefficient of assurance of R^2.

Table 1 Properties of materials used

S.No	Properties	Natural coarse aggregate (NCA)	Recycled coarse aggregate (RCA)	Fine aggregate (FA)	Cement	Super plasticizer (SP)
1	Specific surface area (m^2/kg)	-	-	-	331	-
2	Initial setting time (min)	-	-	-	30	-
3	Final setting time (min)	-	-	-	520	-
4	28d Compressive Strength (MPa)	-	-	-	56.5	-
5	Fineness Modulus (FM)	7.23	7.72	1.92	-	-
6	Specific gravity (SG)	2.76	2.5	2.54	3.13	1.2
7	Water Absorption (WA) (%)	0.36	1.95	4	-	-
8	Impact Value (%)	30	34	-	-	-
9	Crushing Value (%)	18	21	-	-	-

Multi-linear regression (MLR)

MLR is used for researching the functional connection between the predictor variable and response variable components by fitting a multi-linear equation over the data. In contrast to simple linear regression, where a dependent variable and an independent variable relate on a straight line, MLR utilizes multiple independent variables to fit the model in n-measurements though, the number of independent variables is represented by n.

$$Y = \beta_o + \sum_{i=1}^{m} \beta_i x_i + \varepsilon \quad (1)$$

Y = dependent variable
β_0 = constant
β_i = regression coefficient (i=1,2,3,. . . ,n)
X_i = independent variable
ε = error term

This model depends on the mean square error that decides the variation between the actual and computed values. This strategy changes the coefficients of the independent variables utilizing optimization techniques and proceeds with the methodology until the model is viewed as the best fit. Figure 2 shows the schematic representation of multi-linear regression model.

Extreme gradient boosting (XGB)

XGB is a decision tree-based ensemble model that predicts exact outcomes by combining the outcomes got from a few weaker models. It is a supervised learning technique and likely could be utilized to determine various complex issues like regression, classification, and ranking (Ahmad et al. 2021). XGB depends on a gradient boosting framework that employs tree ensembles but unlike gradient boosting, XGB improves the approximation utilizing Newton's boosting method and advanced regularization as inferred (Chen and Guestrin 2016). The primary benefit of utilizing XGB or some other tree-based algorithm is its capacity to model the non-linear interactions between the features as explained (Caruana and Niculescu-Mizil 2006).

$$Obj = L(\theta) + \Omega(\theta) \quad (2)$$

Where
L = training loss function
Ω = regularization term

Since it is a regression problem, for the loss function, mean squared error is used and is given by

$$L(\varphi) = \sum_i l(\hat{y}, y) + \sum_k \Omega(fk) \quad (3)$$

The difference between the prediction $\hat{y}$ and the target y measures the differentiable convex loss function which is represented as "l." To avoid overfitting the model, the regularization term is used which controls the complexity.

The complexity in XGB is defined as,

$$\Omega(f_k) = \gamma T + \frac{1}{2}\lambda \|w\|_2^2 \quad (4)$$

Where w and T represent weights and number of leaves or terminal nodes respectively. Figure 3 shows the schematic representation of extreme gradient boost model.

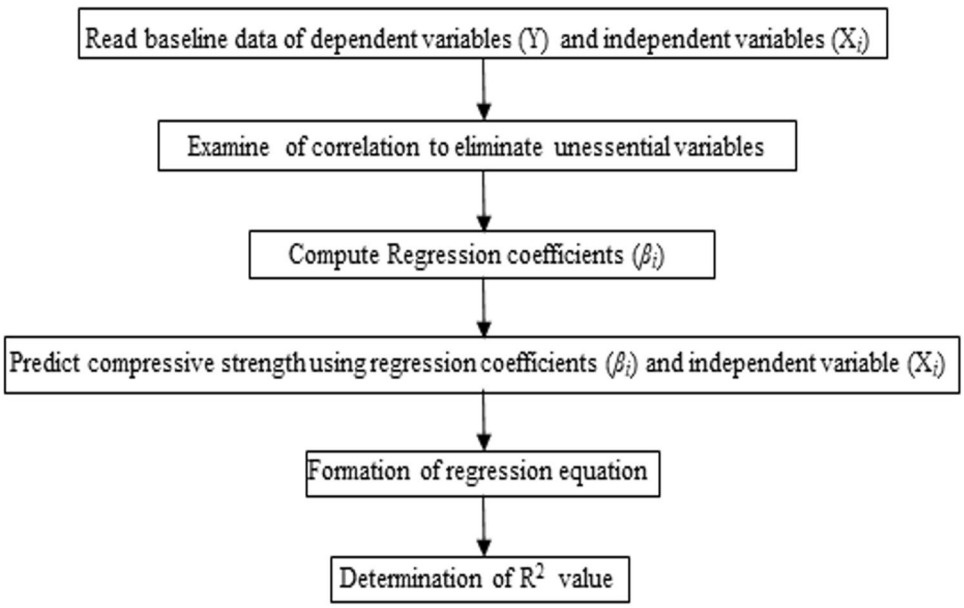

Fig. 2 Flowchart of MLR model

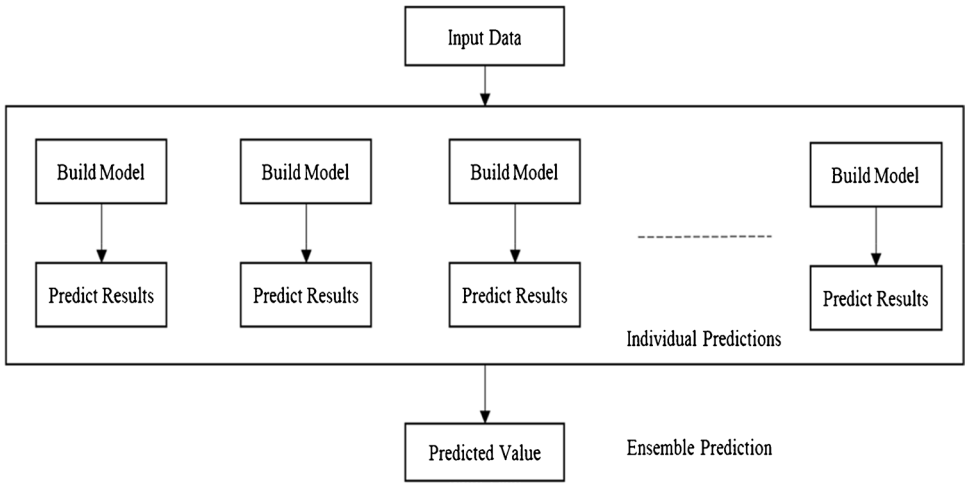

Fig. 3 Flowchart of XGB model

Table 2 Mix proportions of RAC

Mix ID	Material Proportion (%)	W/C	SP	WC	NCA	RCA	FA
1	100% RCA+0%NCA	0.48	0	237.734	0	1130.564	557.729
2	75%RCA+25%NCA	0.48	0	209.9	310.518	847.995	557.729
3	50% RCA+50%NCA	0.48	0	195.37	621.037	575.405	557.729
4	25% RCA+75%NCA	0.48	0	200.98	931.56	282.645	557.729
5	0%RCA+100%NCA	0.48	0	219.718	1242.08	0	557.729
6	100% RCA+0%NCA	0.4	0	207.295	0	1290.32	556.157
7	75%RCA+25%NCA	0.4	0	179.29	332.96	909.21	556.157
8	50% RCA+50%NCA	0.4	0	174.46	665.925	606.14	556.157
9	25% RCA+75%NCA	0.4	0	169.688	998.872	303.07	556.157
10	0%RCA+100%NCA	0.4	0	187.985	1331.838	0	556.157
11	100% RCA+0%NCA	0.3	1.5	151.235	0	1308.92	546.884
12	75%RCA+25%NCA	0.3	1.5	140.79	359.511	981.72	546.884
13	50% RCA+50%NCA	0.3	1.5	135.62	719.004	654.46	546.884
14	25% RCA+75%NCA	0.3	1.5	130.407	1078.506	327.23	546.884
15	0%RCA+100%NCA	0.3	1.5	147.981	1138.01	0	546.884

Description of data set and preparation

An experiment was performed on recycled coarse aggregate ratio of 0%, 25%, 50%, 100% with 400kg/m^3 of cement content, varying w/c (0.3, 0.4, and 0.48) and SP dosage. Concrete was made by utilizing potable water. All the concrete mixes were prepared and cured with legitimate conditions. The testing of samples was done at a curing time of 7, 28, and 56 days. Table 2 shows the mix proportion of RAC.

The input parameters for creating models incorporate W/C, SP, FA, RCA, NCA, AGE and water content (WC). The target parameter and output acquired are assigned as experimental and predicted CSC respectively. Table 3 shows the range and Table 4 indicates the statistical parameters of input and output. For the succeeding step, on account of assessment models MLR, and XGB were selected and the approximation of CSC has been accomplished.

Table 3 Range of input and output parameters

S.No	Input/output	Components/ Parameters	Minimum	Maximum
1	Input	W/C	0.3	0.48
2	Input	SP (%)	0	1.5
3	Input	FA	546.884	557.729
4	Input	NCA	0	1331.838
5	Input	RCA	0	1308.92
6	Input	WC	130.407	237.734
7	Input	AGE	7	56
8	Output (f_{cu})	Compressive strength (MPa)	25.57	61.60
9	Output (f_{cyl})	Compressive strength (MPa)	19.94	49.28

Table 4 Statistical Parameters input and output parameters

Index	Variable	Range	Mean (μ)	Median	Variance (σ^2)	Standard deviation (σ)
1	W/C	0.18	0.39	0.39	0.008	0.09
2	SP (%)	1.5	0.75	0.75	0.5625	0.75
3	FA	10.845	552.3065	552.3065	29.4	5.41
4	NCA	1331.838	665.5919	665.5919	443448.12	665.919
5	RCA	1308.92	654.46	654.46	428317.8	654.46
6	WC	107.327	184.0705	184.0705	2879.39	53.66
7	AGE	49	31.5	31.5	600.25	24.5
8	f'_{cu} (MPa)	36.03	43.585	43.585	324.720	18.02
9	f'_{cyl} (MPa)	29.34	34.61	34.61	215.208	14.67

Experimental work

Mechanical properties of the mixes were assessed with 270 specimens using 150mm cubes for cube compressive strength, 270 specimens using 100x200mm cylinders for cylinder compressive strength, 270 specimens using 100x200mm cylinders for split tensile strength, 90 specimens using 100x100x500mm prism for flexural strength and 180 specimens using 100x200mm cylinders for elastic modulus has been used. Table 5 shows the specimen and experiment details.

SEM analysis

The SEM examination was led for the RAC at 56 days. Concrete samples were cut down into $10mm^3$ size pieces. To stop the hydration interaction, the test specimens were placed in the oven at 95 ± 5°C for 24 h. After drying the specimens were cleaned utilizing a 500-grade silicon carbide paper and put in a desiccator to block carbonation. Then, at that point, the cleaned tests were sputter covered with carbon before testing. The SEM examination was completed utilizing the Tescan VEGA-3 scanning electron microscope. Three specimens were prepared and tested for w/c of 0.3 which showed better results compared to other mixes to recognize their morphology.

Results and discussions

Data-driven models

Each of the models was assembled utilizing Python with algorithms used from various packages. The paper started the disclosures of an investigation to anticipate the concrete compressive utilizing the strategies MLR, and XGB. The MLR model was assembled utilizing the Linear Regression model in the scikit-learn bundle by the Pedregosa Scikit-learn (2011). Loading the dataset and preparing the model took the least amount of time. Figure 4 (a) and (b) shows the Predictive precision result and the Predictive Vs Original cube compressive strength results for the MLR model respectively. Figure 5 (a) and (b) shows the Predictive precision result and the Predictive Vs Original cylinder compressive strength results for the MLR model respectively.

XGB was executed by the python platform utilizing the XGBoost package as illustrated (Chen and Guestrin 2016). Figure 6(a) and (b) shows the Predictive precision result and the Predictive Vs Original cube compressive strength results for the XGB model respectively. Figure 7 (a) and (b) shows the Predictive precision result and the Predictive Vs Original cylinder compressive strength results for the XGB model respectively.

Table 5 Specimen and experiment details

Name of the Experiment	IS code used	Specimen type	Size of the Specimen (mm)	No of the specimens tested	Testing Ages (days)
Cube Compressive Strength	IS- 516 (2004)	Cube	150x150x150	270	7,28, and 56
Cylinder Compressive Strength	ASTM-C39 (2018)	Cylinder	100x200	270	7,28, and 56
Splitting Tensile Strength	ASTM-C496 (2017)	Cylinder	100x200	270	7,28, and 56
Flexural Strength	ASTM-C78 (2018)	Prism	100x100x500	90	7,28, and 56
Modulus of Elasticity	ASTM-C469 (2014)	Cylinder	100x200	180	7,28, and 56

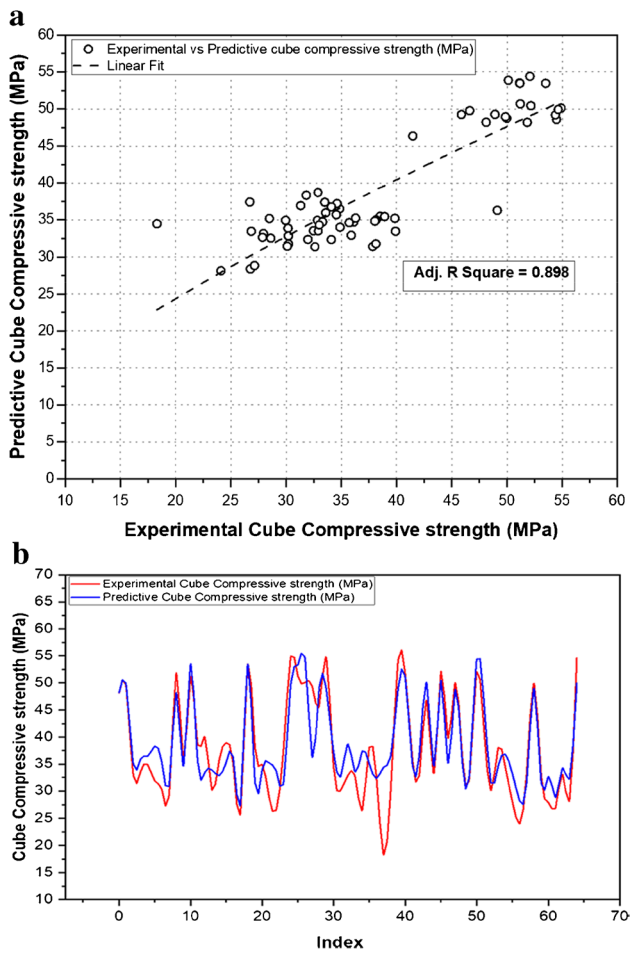

Fig. 4 **(a)** Predictive accuracy result for cube compressive strength-MLR model. **(b)** Predictive Vs Original cube compressive strength results for the MLR model

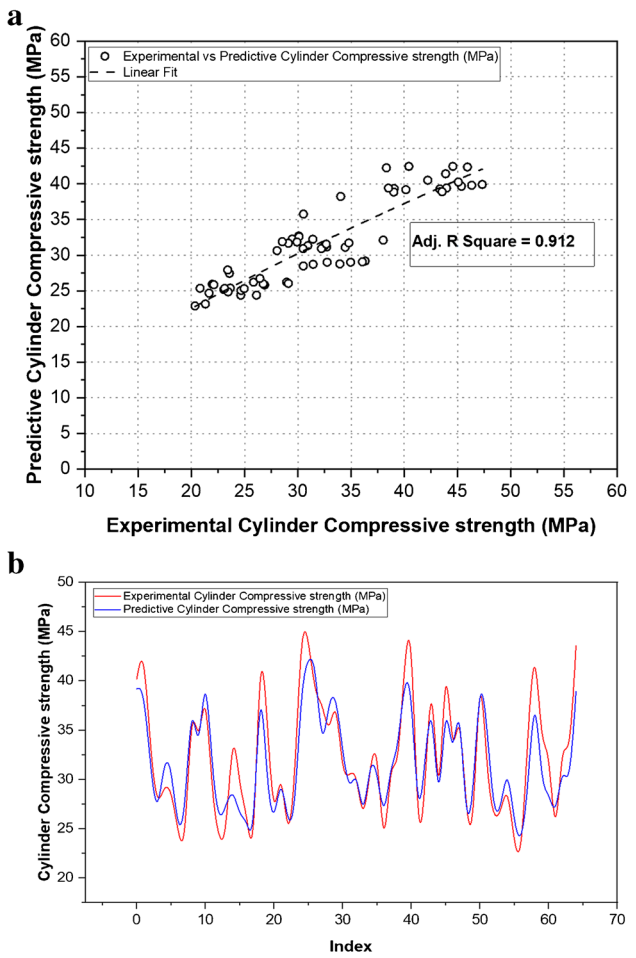

Fig. 5 **(a)** Predictive precision result for cylinder compressive strength-MLR model. **(b)** Predictive Vs Original cylinder compressive strength results for the MLR model

Based on the models that were built, it was noticed that XGB for the prediction of cylinder compressive strength had the highest accuracy compared to the prediction of cube compressive strength. Similarly, MLR for the prediction of cylinder compressive strength had more accuracy compared to the prediction of cube compressive strength. This outcome was observed not just in the correlation coefficient but also for the other statistical coefficients like R^2, RMSE, MAPE, MAE, AAE, MSE, VAF, and ME. Table 6 shows the comparison results for correlation and statistical coefficients.

For the prediction of cylinder compressive strength (f_{cyl}) R^2 value for XGB was found to be 0.5% greater than MLR (f_{cyl}). For the prediction of cube compressive strength (f_{cu}) MLR was found to be 0.67% greater than XGB. The obtained results of RMSE for XGB (f_{cyl}) was 1.4% lesser than MLR model. Whereas, the RMSE for XGB (f_{cu}) was 1.07% greater than MLR model. MAE for XGB (f_{cyl}) was 3.96% lesser than MLR model and XGB (f_{cu}) was 0.85% greater than than MLR model. MAPE for XGB (f_{cyl}) was 1.2% lesser than MLR model and XGB (f_{cu}) was 2.3% greater than MLR model. Values of AAE, MSE, ME, and VAF for XGB (f_{cyl}) showed almost accurate in contrast with other models.

Influence of RAC in strength improvement

The strength improvement in the RCA mix as indicated in Table 7 was evaluated using 7, 28, and 56 days compressive strength results, particularly 56 days compressive strength of each RCA mix was taken as a source value for the estimation. For the W/C of 0.48, the mix containing 100%, 75%, and 50% RCA for 7d acquired practically 66% of its compressive strength and 25% of RCA was 66.4% whereas, the mix containing only NCA gained 66.5% of compressive strength which was found almost same. For 28d, 100%, 75%, 25%, 50% of RCA, and 100% NCA was gained 87% of compressive strength. For the W/C of 0.4, the mix containing 100%, and 75% RCA for 7d gained almost 69% of its

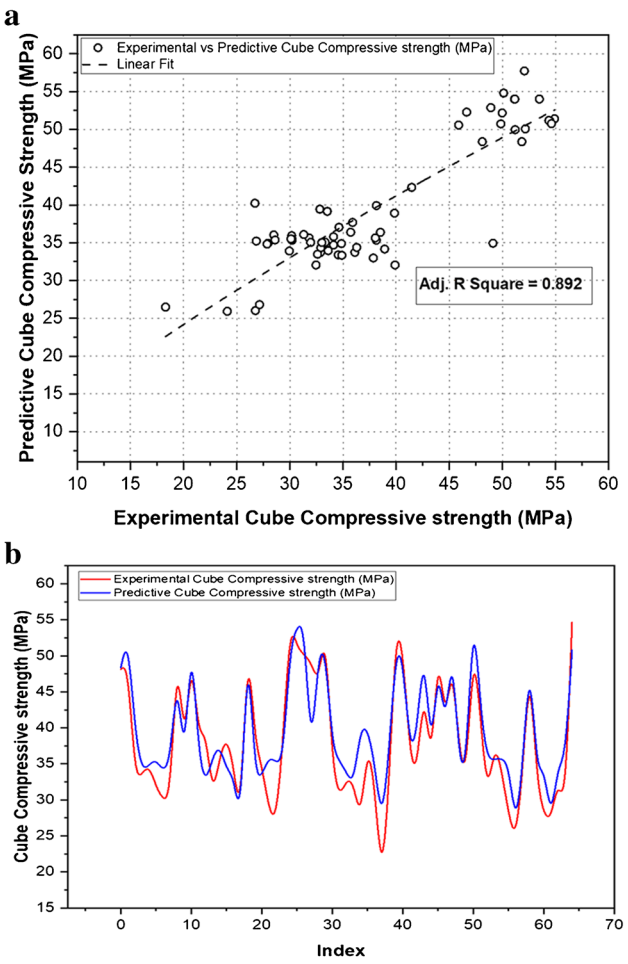

Fig. 6 **(a)** Predictive precision result for cube compressive strength-XGB model. **(b)** Predictive Vs Original cube compressive strength results for the XGB model

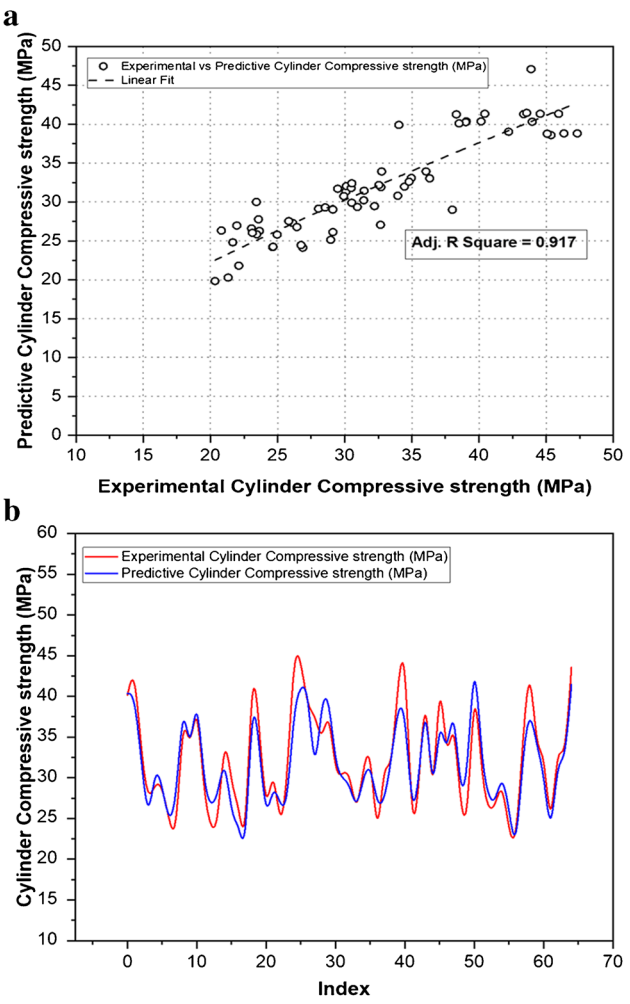

Fig. 7 **(a)** Predictive precision result for cylinder compressive strength-XGB model. **(b)** Predictive Vs Original cylinder compressive strength results for the XGB model

compressive strength, whereas 50% 25% of RCA and 100% NCA was 69.5% compressive strength. Also, 100% and 75% RCA for 28d gained almost 86% of its compressive strength, and 50% 25% of RCA and 100% NCA gained 86.3% which was found almost the same. For the W/C of 0.3 with SP of 1.5%, 100%RCA was found to be around 74% and 28d was found to be around 96% of compressive strength. 75%, 50%, 25% of RCA and 100% of NCA was found to be around 75% also, 28d for 75%, 50%, 25% of RCA was found almost 96 to 97%, whereas, 100%NCA for 28d gained 97% of compressive strength.

Hardened density

The density of RAC mixes was observed for 7, 28, and 56 days for the W/C 0.48, 0.4, and 0.3. For W/C of 0.48, 100%NCA density for 7d, 28d and 56d was 2526kg/m^3, 2532kg/m^3, and 2541kg/m^3 respectively. 7d hardened density for replacement ratio was found between the ranges of 2418kg/m^3 to 2495kg/m^3 which was 4.27% to 1.23% lower than the NCA. 28d hardened density for replacement ratio was found between the ranges of 2423 to 2487kg/m^3 which was 4.3 to 1.78% lower than the NCA. 56d hardened density

Table 6 Correlation and statistical coefficients comparison

Statistical Measure	MLR		XGB	
	Cube	Cylinder	Cube	Cylinder
R^2	0.898	0.912	0.892	0.917
RMSE	4.5210	3.3883	4.5701	3.3414
MAE	1.8642	1.6777	1.8802	1.6137
MAPE	5.1137	5.0604	5.2355	5.0008
AAE	0.053	0.043	0.054	0.04
MSE	20.440	11.480	20.886	11.165
VAF	0.7685	0.8055	0.7799	0.8092
ME	4.38	4.01	4.38	4.01

Table 7 Strength improvement in RAC mix at different age periods

Mix ID	Material Proportion (%)	W/C	SP	f7/f56	f28/f56	f56/f56
1	100% RCA+0%NCA	0.48	0	0.663	0.869	1
2	75%RCA+25%NCA	0.48	0	0.663	0.869	1
3	50% RCA+50%NCA	0.48	0	0.663	0.869	1
4	25% RCA+75%NCA	0.48	0	0.664	0.870	1
5	0%RCA+100%NCA	0.48	0	0.665	0.871	1
6	100% RCA+0%NCA	0.4	0	0.692	0.859	1
7	75%RCA+25%NCA	0.4	0	0.694	0.860	1
8	50% RCA+50%NCA	0.4	0	0.695	0.863	1
9	25% RCA+75%NCA	0.4	0	0.695	0.863	1
10	0%RCA+100%NCA	0.4	0	0.695	0.863	1
11	100% RCA+0%NCA	0.3	1.5	0.748	0.964	1
12	75%RCA+25%NCA	0.3	1.5	0.750	0.965	1
13	50% RCA+50%NCA	0.3	1.5	0.751	0.966	1
14	25% RCA+75%NCA	0.3	1.5	0.752	0.968	1
15	0%RCA+100%NCA	0.3	1.5	0.753	0.970	1

for replacement ratio was found between the ranges of 2432 to 2503kg/m^3 which was 4.28% to 1.49% lower than the NCA. For W/C of 0.4, 100%NCA density for 7d, 28d and 56d was 2581kg/m^3, 2590kg/m^3, and 2580kg/m^3 respectively. 7d hardened density for replacement ratio was found between the ranges of 2413kg/m^3 to 2544kg/m^3 which was 6.5 to 1.43% lower than the NCA. 28d hardened density for replacement ratio was found between the ranges of 2393 to 2550kg/m^3 which was 7.6% to 1.54% lower than the NCA. 56d hardened density for replacement ratio was found between the ranges of 2398 to 2542kg/m^3 which was 7.05 to 1.47% lower than the NCA. For W/C of 0.3, 100%NCA density for 7d, 28d and 56d was 2539kg/m^3, 2546kg/m^3, and 2556kg/m^3 respectively. 7d hardened density for replacement ratio was found between the ranges of 2430 to 2507kg/m^3 which was 4.3 to 1.3% lower than the NCA. 28d hardened density for replacement ratio was found between the ranges of 2437 to 2501kg/m^3 which was 4.3% to 1.8% lower than the NCA. 56d hardened density for replacement ratio was found between the ranges of 2447 to 2518kg/m^3 which was 4.3 to 1.5% lower than the NCA. Due to the high w/c (0.48) and minimum w/c of 0.3 with SP of 1.5%, the 56days density increased marginally compared with 28d values. The intermittent high W/C of 0.4 also without SP, the density has marginally decreased in contrast to 28d results. Figure 8 shows the hardened density of RAC mixes.

Compressive strength—cube

Compressive strength for the cube, the RAC mixes noticed at different testing age periods as indicated in Fig. 9. For the w/c of 0.48, 56d cube compressive strength ranges from 38.57MPa to 43.34MPa which was found 13.2% and 2.5% lower than NAC mix. 28d compressive strength was observed from 33.61 to 37.72MPa which was 13% and 2.4% lower than the NAC mix. 7d compressive strength was observed between 25.57 and 28.77MPa from 13 and 2.6% lower than the NAC mix. For the w/c of 0.4, 56d compressive strength ranges from 38.53MPa to 42.79MPa which was found 15% and 5.6% lower than the NAC mix. 28d compressive strength was observed from 33.11 to 36.75 MPa which was 15 % and 6% lower than the NAC mix. 7d compressive strength was observed between 26.77 to 29.74 MPa from 14.6% and 5% lower than the NAC mix. For the w/c of 0.3, 56d compressive strength ranges from 53.53MPa to 59.86MPa which was found 13% and 2.8% lower than the NAC mix. 28d compressive strength was observed from 51.41 to 57.84 MPa which was 13.8% and 3% lower than the NAC mix. 7d compressive strength was observed between 40.16 and 44.98 MPa from 13% and 2.6% lower than the NAC mix. The decrease in compressive strength with the usage of over 30% RCA was normally seen in numerous studies (Ahmed 2013; Yong Ho et al., 2013; Sivakumar 2014). The decrease was probably because of the adhered in RA, which affects the porous ITZ hence becomes the weakest point in RAC as evident (Etxeberria et al. 2007; Poon et al. 2004). Figure 10 shows the tested specimens prepared to compressive strength.

Compressive strength—cylinder

Compressive strength for cylinder, the RAC mixes noticed at different testing age period as indicated in Fig. 11. For the w/c of 0.48, 56d cylinder compressive strength ranges from 30.08MPa to 33.8 MPa which was found 15% and 5% lower than the NAC mix. 28d compressive strength was observed from 26.22 to 29.42MPa which was 15% and 4.8% lower than the NAC mix. 7d compressive strength was observed

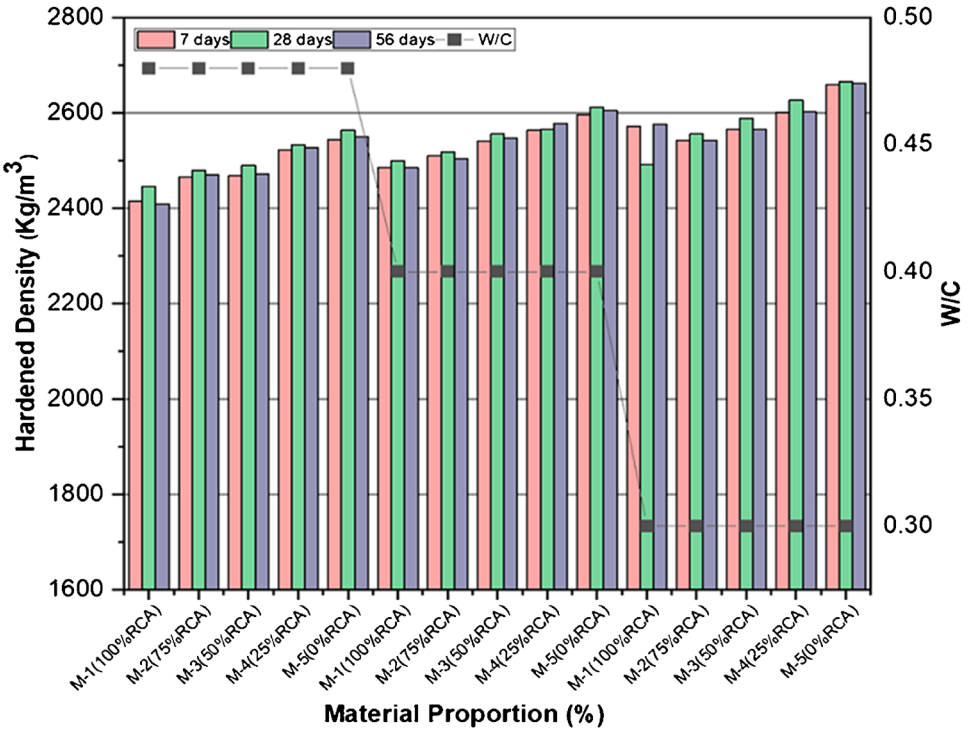

Fig. 8 Hardened density of RAC mixes

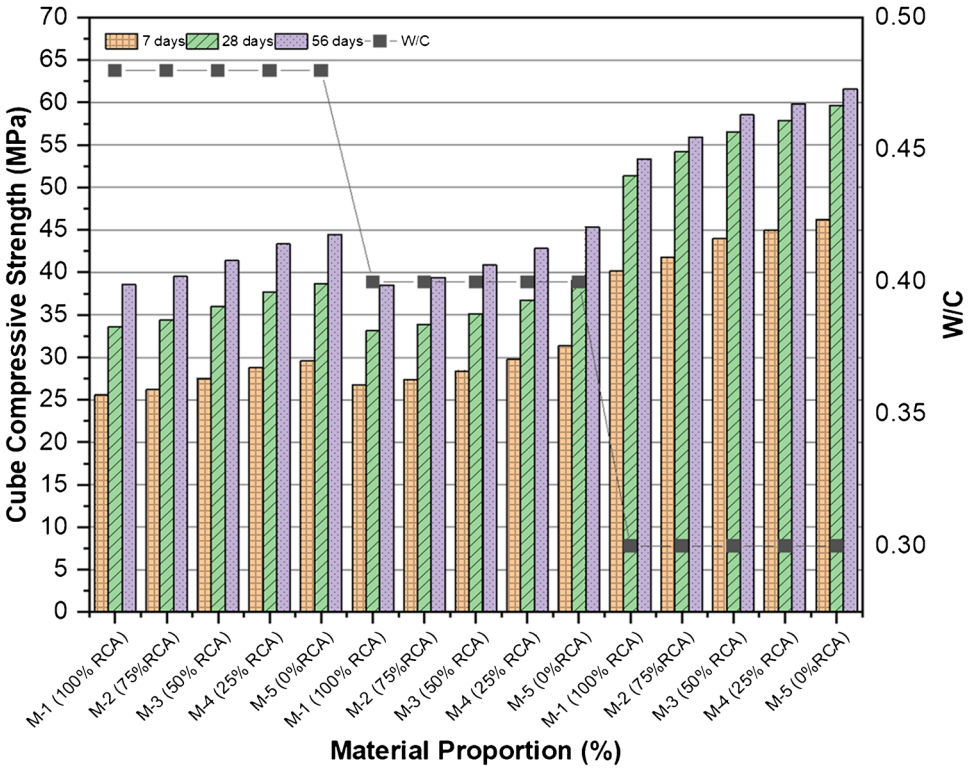

Fig. 9 Cube compressive strength of RAC mixes

between 19.94 to 22.44 MPa from 14.5% and 5% lower than the NAC mix. For the w/c of 0.4, 56d compressive strength ranges from 30.05MPa to 33.38MPa which was found 16% and 7.9% lower than the NAC mix. 28d compressive strength was observed from 25.83 to 28.67 MPa which was 17.4 % and 8.3% lower than the NAC mix. 7d compressive strength was observed between 20.88 to 23.2 MPa from 16.7% and 7.4% lower than the NAC mix. For the w/c

Fig. 10 Tested specimens

of 0.3, 56d compressive strength ranges from 41.6MPa to 46.69MPa which was found 15% and 5.3% lower than the NAC mix. 28d compressive strength was observed from 40.1 to 45.11 MPa which was 15.9% and 5.4% lower than the NAC mix. 7d compressive strength was observed between 31.32MPa to 35.08MPa which was 15% and 5% lower than the NAC mix. the strength reduction (%) of RAC mixes for cube was around 15.3–2.4% and for cylinder, it was around 16.8–11.3%. Same effect has been in the study Yong Ho et al. (2013), in examining the efficient utilization of RAC in structural concrete. It is reasoned that the strength reduction of cylinder specimen is slightly higher than the cube specimens. The strength variation of RAC mixes compared to NAC mixes is inferred in Table 8.

Correlation between the 56d cube and cylinder compressive strength is indicated in Fig. 12. Equation 5 shows a model attained by the non-linear regression with the good correlation coefficient of $R^2 = 0.94145$ to relate the cube (f_{cu}) and cylinder compressive strength (f_{cyl}).

$$Compressivestrengthofcylinder\left(f_{cyl}\right) = 1.23{f_{cu}}^{0.878} \quad (5)$$

Split tensile strength

Split Tensile strength for RAC mixes noticed at different testing age periods as indicated in Fig. 13. For the w/c of 0.48, 56d split tensile strength ranges from 3.214 to 3.611MPa which was found 13% and 2.5% lower than the NAC mix. 28d split tensile strength was observed from 2.801 to 3.143 MPa which was 13% and 2.4% lower than the NAC mix. 7d split tensile strength was observed between 2.131 to 2.397 MPa from 13% and 2.6% lower than the NAC mix. For the w/c of 0.4, 56d split tensile strength ranges from 3.211MPa to 3.566MPa which was found 15% and 5.6% lower than the NAC mix. 28d split tensile strength was observed from 2.759 to 3.063 MPa which was 15 % and 6% lower than the

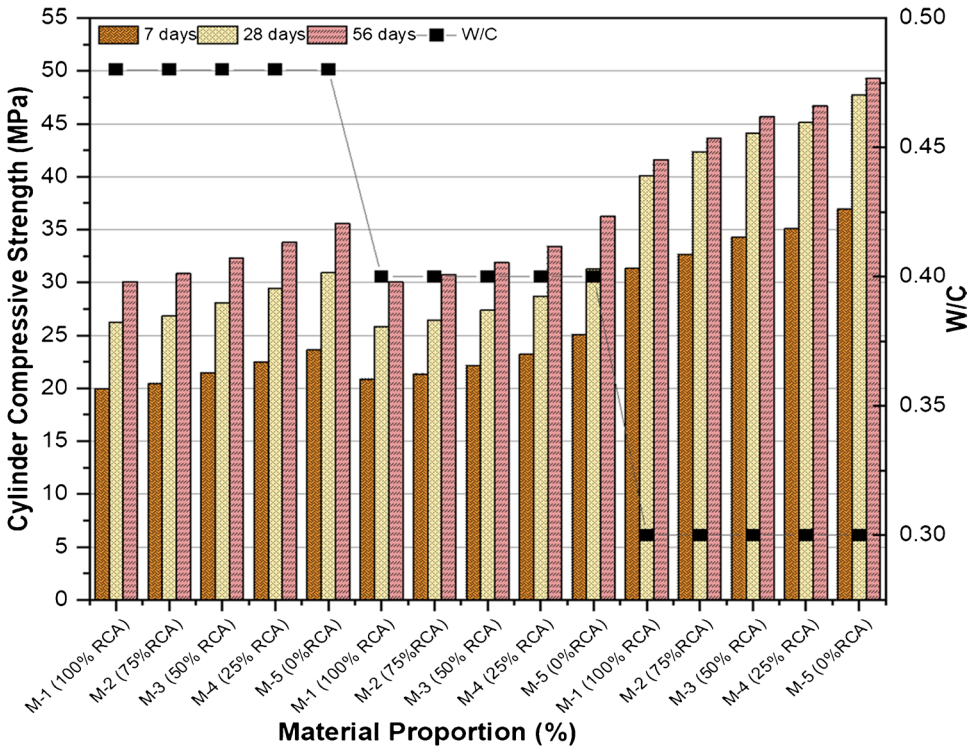

Fig. 11 Cylinder compressive strength of RAC mixes

Table 8 Strength variation (%) in RAC mixes compared to NAC mixes

Material proportion	w/c	f_{cu}(MPa)			f_{cyl}(MPa)			f_{ct}(MPa)			f_{cr}(MPa)			E(GPa)		
		7	28	56	7	28	56	7	28	56	7	28	56	7	28	56
100%RCA	0.48	13.47	13.04	13.2	14.5	15.2	15.4	13.4	13	13.2	6.9	6.9	6.8	8.1	7.9	8
75% RCA		11.3	10.9	11	13.4	13.1	13.3	11.3	10.9	11	5.7	5.6	5.7	6.9	6.8	6.9
50% RCA		6.9	6.9	6.9	9.3	9.3	9.2	6.9	6.9	6.9	3.5	2.9	3.5	4.7	4.8	4.8
25%RCA		2.6	2.4	2.5	5	4.9	4.9	2.6	2.4	2.5	1.5	1.2	1.3	2.5	2.4	2.5
100%RCA	0.4	14.6	15.3	14.9	16.7	17.4	16.2	14.6	15.3	15	7.5	7.9	7.8	8.7	9.1	8.9
75% RCA		12.7	13.4	13	14.9	15.5	15.2	12.7	13.3	13	7.5	6.8	6.7	7.7	8	7.9
50% RCA		9.5	10.1	9.8	11.7	12.4	12	9.5	10	9.8	4.8	5.2	5	6	6.4	6.2
25%RCA		5.1	6	5.6	7.5	8.3	7.9	5.1	6	5.6	2.5	3	2.8	3.8	4.3	4
100%RCA	0.3	13	13.7	13.4	15	15.9	14.9	13	13	13	6.7	7.1	6.9	7.9	8.3	8.1
75% RCA		9.5	9	9.2	11.7	11.2	11.5	9	8	8	4.8	4.6	4.7	6	5.8	5.9
50% RCA		4.7	5.2	4.9	7.1	7.5	7.3	4.8	4.2	1.8	2.4	2.6	2.5	3.6	3.8	3.7
25%RCA		2.5	3	2.8	5.1	5.4	5.3	2.6	4	3.2	1.3	1.5	1.4	2.6	2.8	2.7

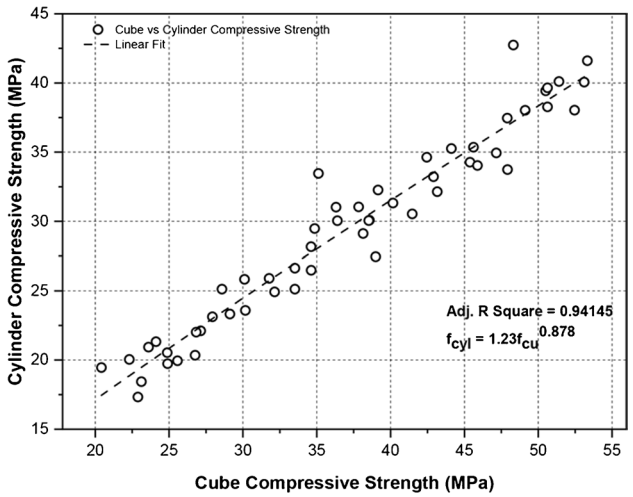

Fig. 12 Correlation between cube and cylinder compressive strength

NAC mix. 7d split tensile strength was observed between 2.231 and 2.479 MPa from 14.6% and 5% lower than the NAC mix. For the w/c of 0.3, 56d split tensile strength ranges from 4.444MPa to 4.81 MPa which was found 13% and 3.2% lower than the NAC mix. 28d split tensile strength was observed from 4.284 to 4.72 MPa which was 13% and 4% lower than the NAC mix. 7d split tensile strength was observed between 3.347MPa and 3.748MPa which was 13% and 2.6% lower than the NAC mix. Since the NCA provides high resistance, the tensile crack which propagates from the mortar is highly restricted in contrast to RCA. A similar effect was noticed in the literature Sivakumar (2014) in exploration with high-performance concrete using RCA.

Correlation between the 56d compressive strength (both cube and cylinder) and split tensile strength is indicated in Fig. 14. Equations 6 and 7 show a model arrived by the non linear regression with the good correlation coefficient of R^2 as 0.9154 and 0.90728 for cylinder (f_{cyl}) and cube (f_{cu}) compressive strength respectively.

$$Splittensilestrengthforcylinder(f_{ct}) = 0.541 f_{cyl}^{0.531} \quad (6)$$

$$Splittensilestrengthforcube(f_{ct}) = 0.565 f_{cu}^{0.483} \quad (7)$$

Flexural strength

Flexural strength for RAC mixes noticed at different testing age period as indicated in Fig. 15. For the w/c of 0.48, 56d flexural strength ranges from 4.347MPa to 4.608MPa which was found 6.8% and 1.3% lower than the NAC mix. 28d flexural strength was observed from 4.058to 4.299 MPa which was 6.8% and 1.2% lower than the NAC mix. 7d flexural strength was observed between 3.54to 3.754MPa from 6.9% and 1.3% lower than the NAC mix. For the w/c of 0.4, 56d flexural strength ranges from 4.345MPa to 4.579MPa which was found 7.8% and 2.8% lower than the NAC mix. 28d flexural strength was observed from 4.028 to 4.244 MPa which was 7.9% and 3% lower than NAC mix. 7d flexural strength was observed between 3.622 to 3.818 MPa from 7.6% and 2.6% lower than the NAC mix. For the w/c of 0.3, 56d flexural strength ranges from 5.112 to 5.416MPa which was found 6.9% and 1.4% lower than the NAC mix. 28d flexural strength was observed from 5.019 to 5.324MPa which was 7.2% and 1.5% lower than the NAC mix. 7d flexural strength was observed between 4.436 MPa to 4.695MPa which was 6.7% and 1.3% lower than the NAC mix. The lesser mechanical properties and elastic modulus of RAC mixes can be the conceivable explanation for the decrease in flexural strength. Because of the lower modulus of elasticity, the RAC goes through more strain when contrasted with

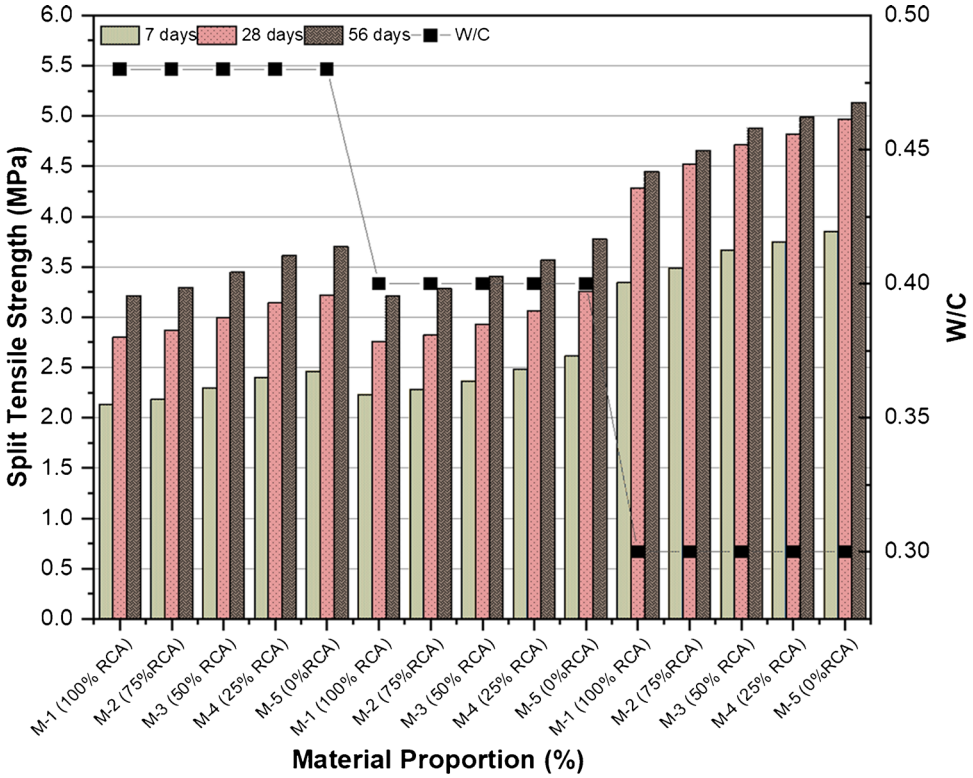

Fig. 13 Split tensile strength of RAC mixes

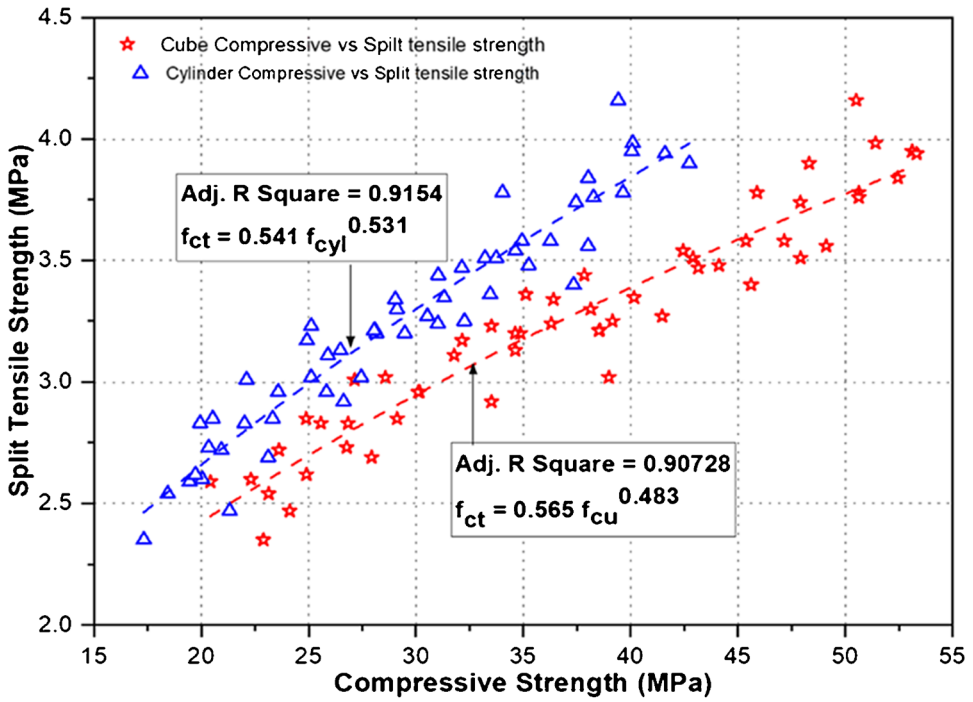

Fig. 14 Correlation between Split tensile and Compressive strength

NAC mixes. In another point of view, voids existing in RAC have a more prominent impact on the tensile strength, more probable on its flexural strength.

Correlation between the 56d compressive strength (both cube and cylinder) and flexural strength is indicated in Fig. 16. Equations 8 and 9 shows a model arrived by the non linear regression with the correlation coefficient of R^2 as 0.90945 and 0.89949 for cylinder (f_{cyl}) and cube (f_{cu}) compressive strength respectively.

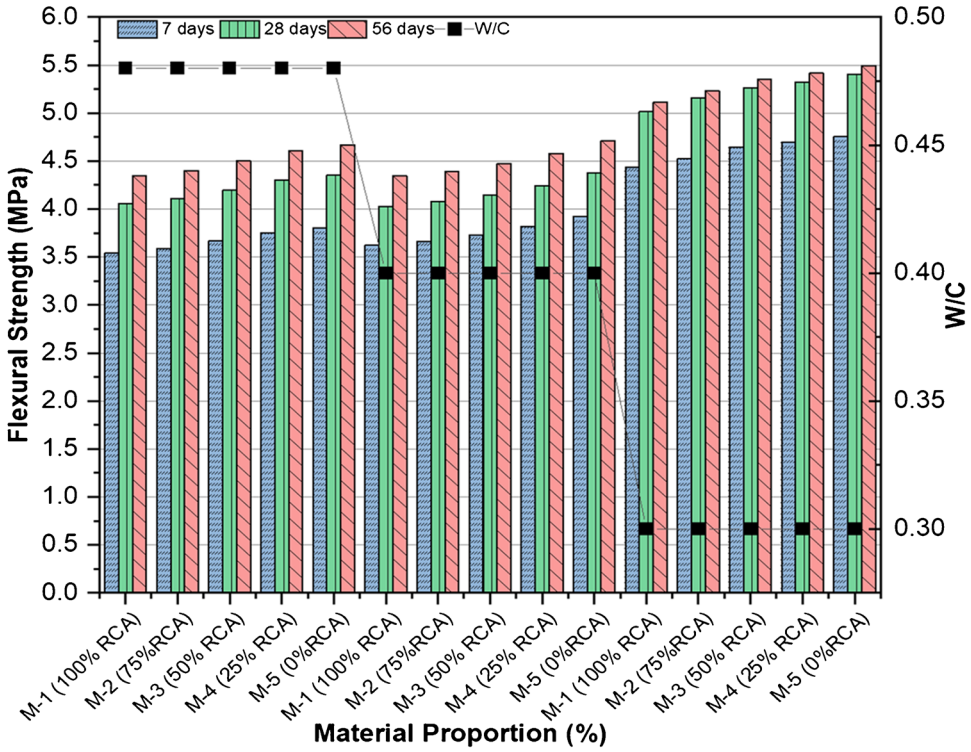

Fig. 15 Flexural strength of RAC mixes

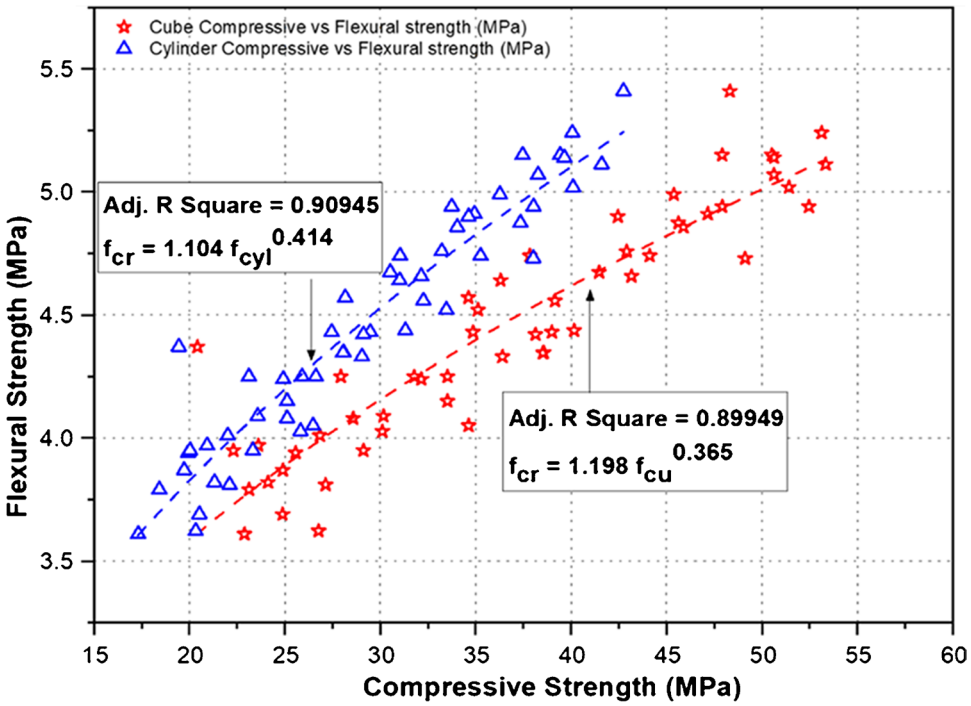

Fig. 16 Correlation between Flexural and Compressive strength

$$Flexuralstrengthforcylinder(f_{cr}) = 1.104 f_{cyl}^{0.414} \quad (8)$$

$$Flexuralstrengthforcube(f_{cr}) = 1.198 f_{cu}^{0.365} \quad (9)$$

Modulus of elasticity

Modulus of Elasticity for RAC mixes noticed at different testing age period as indicated in Fig. 17. For the w/c of 0.48, 56d MOE ranges from 27.42 to 29.07 MPa which was found 8 % and 2.5% lower than the NAC mix. 28d MOE was observed

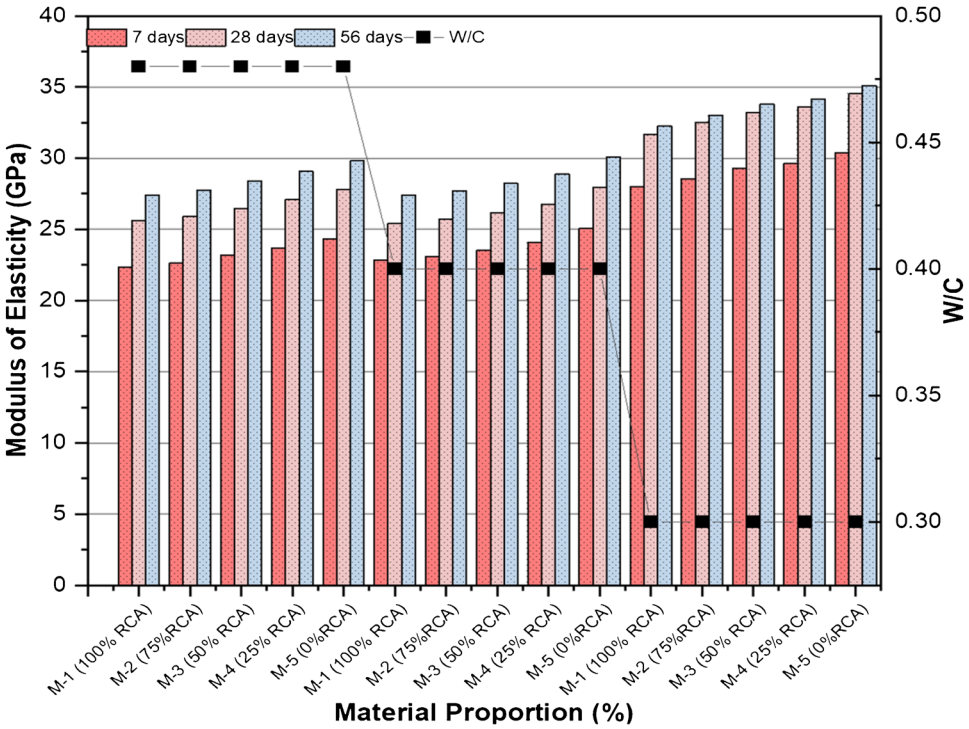

Fig. 17 Modulus of elasticity of RAC mixes

from 25.6 to 27.12MPa which was 7.9% and 2.5% lower than the NAC mix. 7d MOE was observed between 22.329 to 23.684MPa from 8% and 2.6% lower than the NAC mix. For the w/c of 0.4, 56d MOE ranges from 27.41 to 28.885 MPa which was found 8.9% and 4% lower than the NAC mix. 28d MOE was observed from 25.409 to 26.77MPa which was 9.1 % and 4.3% lower than the NAC mix. 7d MOE was observed between 22.847MPa and 24.083MPa from 8.7 % and 3.8% lower than the NAC mix. For the w/c of 0.3, 56d MOE ranges from 32.248MPa to 34.166 MPa which was found 8.1% and 2.6% lower than the NAC mix. 28d MOE was observed from 31.662 to 33.582 MPa which was 8.3% and 2.7% lower than the NAC mix. 7d MOE was observed between 27.984 MPa and 29.615MPa which was 7.9% and 2.5% lower than the NAC mix. It was reasoned that the elastic modulus of RCA was lower in contrast to NCA because of its weak and porous nature. Literature Liu et al. (2011); Fathifazl et al. (2011) also identified the same effect.

Correlation between the 56d compressive strength (both cube and cylinder) and modulus of elasticity is indicated in Fig. 18. Equations 10 and 11 show a model arrived by the non linear regression with the correlation coefficient of R^2 as 0.89003 and 0.89035 for cylinder (f_{cyl}) and cube (f_{cu}) compressive strength respectively. Table 9 shows the relationship between different mechanical properties of RAC.

$$MOEforcylinder(E) = 6.344 f_{cyl}{}^{0.44009} \quad (10)$$

$$MOEforcube(E) = 6.935 f_{cu}{}^{0.3687} \quad (11)$$

Scanning electron microscope

Since the RCA contains adhered mortar have microcracks thus it gets fundamental to inspect the impact of microcrack, pores, and voids present in the concrete. SEM scan for RCA is shown in Fig. 19. Figure 19 (a) shows the pores and cracks present in RCA respectively. Figure 19 (b) shows the porous layer between the aggregate and the cement paste, which forms the wall of the Interfacial Transition Zone (ITZ). Figure 19 (c) shows the dense microstructure of RAC. Since the RCA already has a porous microstructure, water absorption of RAC increases in contrast to NAC.

Limitations and future work

Regardless of the fact that this paper uses machine learning approaches to arrive at models and correlates the mechanical properties of RAC, the work's shortcomings should be addressed. This research is limited to prediction from concrete's various mechanical properties and correlation between them considering only 400kg/m^3 of cement content. Also, the durability, corrosion, abrasion behavior of concrete may be considered in the future work. As concrete is the most extensively utilized substance on the planet after water, it is also advised that its characteristics be incorporated.

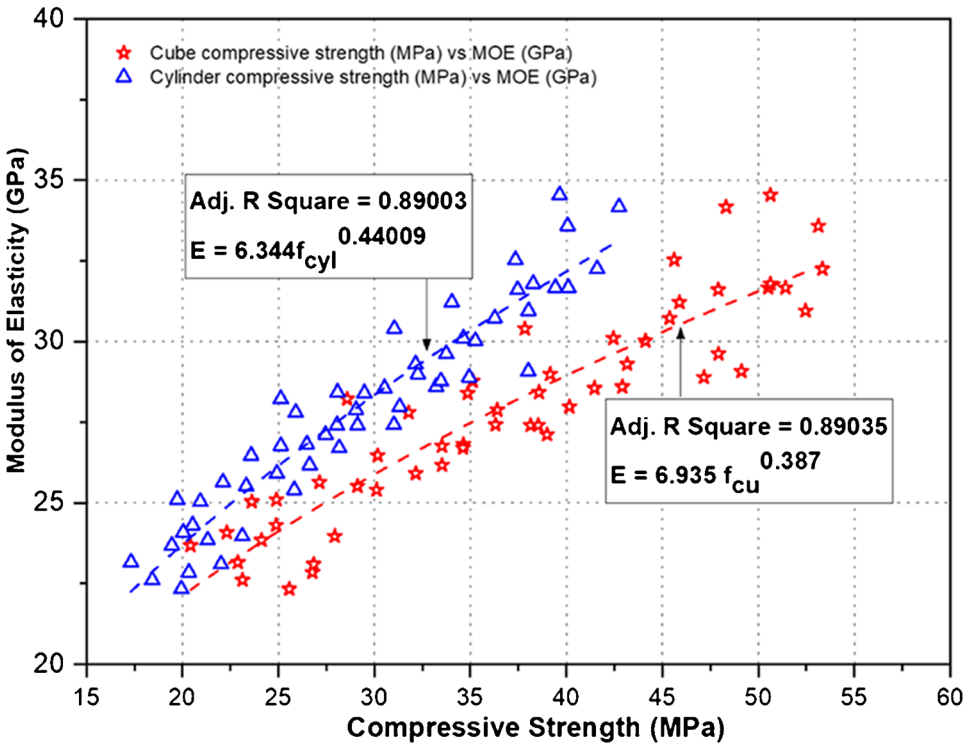

Fig. 18 Correlation between MOE and Compressive strength

Table 9 Relationship between different mechanical properties of RAC

Correlation between	R^2 value	Proposed Models (MPa)
Cube and Cylinder compressive strength	0.94145	$f_{cyl} = 1.23\ f_{cu}^{0.878}$
Split tensile and Compressive strength	$f_{cyl} = 0.9154$ $f_{cu} = 0.90728$	$f_{ct} = 0.541\ f_{cyl}^{0.531}$ $f_{ct} = 0.565\ f_{cu}^{0.483}$
Flexural and Compressive strength	$f_{cyl} = 0.90945$ $f_{cu} = 0.89949$	$f_{cr} = 1.104\ f_{cyl}^{0.414}$ $f_{cr} = 1.198\ f_{cu}^{0.365}$
MOE and Compressive strength	$f_{cyl} = 0.89003$ $f_{cu} = 0.89035$	$E = 6.344\ f_{cyl}^{0.44009}$ $E = 6.935\ f_{cu}^{0.3687}$

Other algorithm based machine learning techniques such as artificial neural network, support vector machine, stochastic gradient boosting, nearest neighbors and program based genetic programming may also be utilized as only Multi linear regression and extreme gradient boosting is described in this paper. Environmental effects on concrete qualities should also be predicted using machine learning approaches. Extreme gradient boosting can be used to obtain great accuracy in both experimental and predicted results.

Conclusions

Concrete compressive strength was predicted and their results were compared using data-driven models such as multilinear regression, and extreme gradient boosting. Results demonstrate that the experimental cylinder compressive strength values of XGB have greater predictions of 0.5% than those of the MLR model. Especially results from establishing an XGB for f_{cyl}, illustrate a good degree of coherency between predicted and actual output values. The obtained cylinder compressive strength results of RMSE, MAE, and MAPE values of XGB were found to be 3.3414, 1.6137, and 5.0008 that are small enough which indicates the estimates are most precise in comparison to MLR. Regarding the fit of a model R^2, for f_{cyl}, the accuracy of XGB was found to be 0.917. Although the R^2 for f_{cyl}, the value of MLR was found greater than 0.9

From the data-driven models, for both accurate and easework, XGB and MLR are used for concrete compressive strength prediction. From this study, it is inferred that the tree-based algorithm was able to perform better regression for f_{cyl} than other algorithms.

Correlations between the various mechanical properties of RAC mixes were established with a good correlation coefficient ranges around 0.899 to 0.941.

Due to the porous structure and micro-cracks present in RCA, the percentage of water absorption increased which

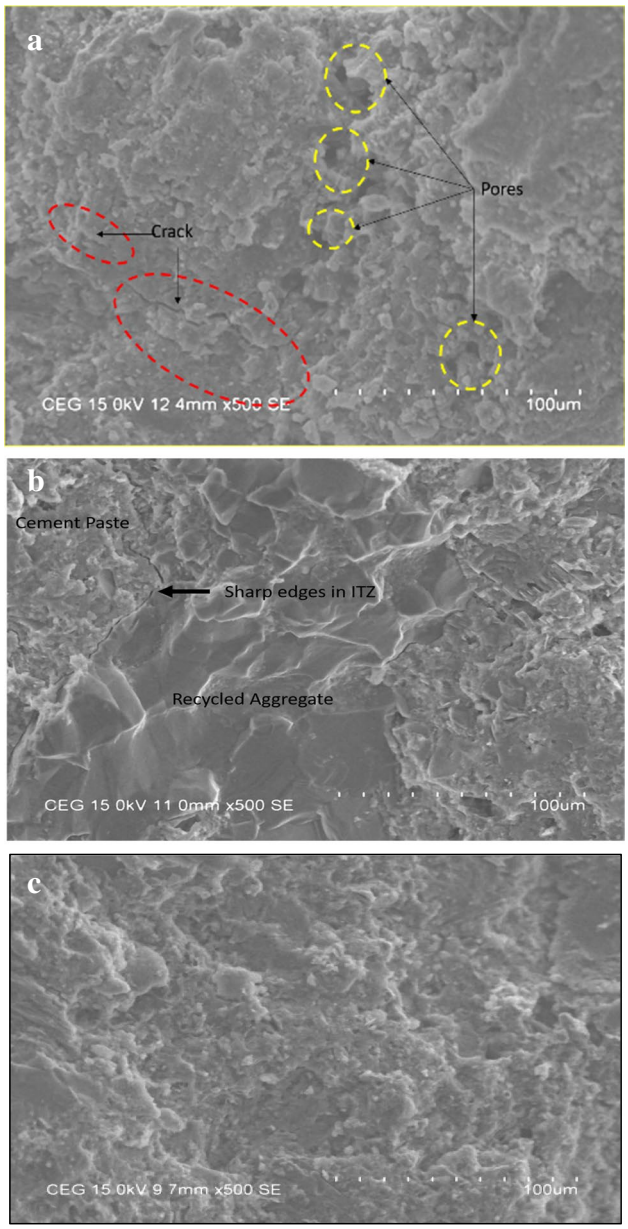

Fig. 19 **(a)** Pores and Cracks in RCA. **(b)** Aggregate and cement interaction. **(C)** Dense Microstructure of RCA

showed an adverse impact on the properties of RAC mixes. But the usage of superplasticizer conplast SP 430 effectively controlled and increased the mechanical properties of RAC. For the w/c of 0.3 with SP of 1.5%, 25% replacement of RCA showed greater results as compared to other w/c. It was recorded that cube compressive strength (2.8% lesser), cylinder compressive strength (5.2% lesser), Split tensile strength (3.2% lesser), flexural strength (1.4% lesser), and elastic modulus (2.6% lesser) than normal aggregate concrete.

Although for other w/c, 25% replacement of RCA showed better results and 100% replacement of RCA with optimum results which recorded cube compressive strength as (8 to 10 % variation), cylinder compressive strength as (10 to 12%) Split tensile strength as (8–10% variation), flexural strength as (4–5% variation), and elastic modulus as (5–6% variation).

For 100% replacement of RCA, 28th day cube compressive strength (f_{cu}) for was found to be 53.33MPa and 28th day cylinder compressive strength (f_{cyl}) was found to be around 40MPa. Hence, it is recommended to be used for all structural applications.

The RAC model which employs MLR and XGB can be employed successfully without requiring a considerable investment of time and money, as in the scenario with long-term experiments.

Author contribution Both the authors contributed equally to this work.
Conceived the ideas and experimental ideas of the study.
Performed the experiments and data were collected.
Data analysis and interpretation were done.
The Paper has been written by the corresponding author.

Data availability Data for the experimental results are available with the authors and can be provided for review purposes.

Declarations

Consent to participate Both the authors agree with their consent to participate in the research.

Consent for publication Both the authors agree with their consent for the publication.

Conflict of interest The authors declare that they have no competing interests.

References

Ahmad A, Farooq F, Niewiadomski P, Ostrowski K, Akbar A, Aslam F, Alyousef R (2021) Prediction of Compressive Strength of Fly Ash Based Concrete Using Individual and Ensemble Algorithm. Materials 14:794. https://doi.org/10.3390/ma14040794

Ahmed SFU (2013) "Properties of Concrete Containing Construction and Demolition Wastes and Fly Ash". Journal of materials in civil engineering, volume 25 issue 12, https://doi.org/10.1061/(ASCE)MT.1943-5533.0000763

Ajdukiewiez A, Kliszczewicz A (2002) Influence of recycled aggregates on mechanical properties of HS/HPC. Cement Concr Compos 24:269–279. https://doi.org/10.1016/S0958-9465(01)00012-9

Akbar A, Liew KM (2020) Assessing recycling potential of carbon fiber reinforced plastic waste in production of eco-efficient cement-based materials. J Clean Prod 274:123001

Almusawi AM, Mehrath HJ, Qasim TA, Shallal MA (2020) Effect of Cement Content on Compressive and Bonding Strength with Steel Bar Reinforcement. Mater Sci Eng 870:012112. https://doi.org/10.1088/1757-899X/870/1/012112

Angulo SC, Ulsen C, John VM, Kahn H, Cincotto MA (2009) Chemicalmineralogical characterization of C&DW recycled aggregates from SãPaulo Brazil. Waste Manage 29(2):721–730. https://doi.org/10.1016/j.wasman.2008.07.009

ASTM C39 (2018) Standard Test Method for Compressive Strength of Cylindrical Concrete Specimens. ASTM International, West Conshohocken

ASTM C469 (2014) Standard Test Method for Static Modulus of Elasticity and Poisson's Ratio of Concrete in Compression. ASTM International, West Conshohocken

ASTM C496 (2017) Standard Test Method for Splitting Tensile Strength of Cylindrical Concrete Specimens. ASTM International, West Conshohocken

ASTM C78 (2018) Standard Test Method for Flexural Strength of Concrete (Using Simple Beam with Third-Point Loading). ASTM International, West Conshohocken

Aydogmus HY, Erdal HI, Karakurt O, Namli E, Turkan YS, Erdal H (2015) A comparative assessment of bagging ensemble models for modeling concrete slump flow. Comput Concr 16:741–757

Belén GF, Fernando MA, Diego CL et al (2011) Stress–strain relationship in axial compression for concrete using recycled saturated coarse aggregate. Constr Build Mater 25(5):2335–2342. https://doi.org/10.1016/j.conbuildmat.2010.11.031

Bilim C, Atis CD, Tanyildizi H, Karahan O (2009) Predicting the compressive strength of ground granulated blast furnace slag concrete using artificial neural network. Adv Eng Soft 40(5):334–340. https://doi.org/10.1016/j.advengsoft.2008.05.005

Caruana R, Niculescu-Mizil A (2006) An empirical comparison of supervised learning algorithms. In: Proceedings of the 23rd international conference on Machine learning. ACM, pp 161–168, https://doi.org/10.1145/1143844.1143865

Chen T, Guestrin C (2016) XGBoost: A Scalable Tree Boosting System in Proceedings of the 22nd ACM SIGKDD. International Conference on Knowledge Discovery and Data Mining, KDD, ACM, New York, USA, pp. 785–794

Corinaldesi V (2010) Mechanical and elastic behaviour of concretes made of recycled-concrete coarse aggregates. Constr Build Mater 24(9):1616–1620. https://doi.org/10.1016/j.conbuildmat.2010.02.031

Corinaldesi V, Moriconi G (2009) Behaviour of cementitious mortars containing different kinds of recycled aggregate. Constr Build Mater 23(1):289–294. https://doi.org/10.1016/j.conbuildmat.2007.12.006

Deepa C, SathiyaKumari K, PreamSudha K (2010) Prediction of the compressive strength of high-performance concrete mix using tree-based modeling. Int J Comput Appl 6(5):18–24

Donga W, Huanga Y, Lehanea B, Maa G (2020) XGBoost algorithm-based prediction of concrete electrical resistivity for structural health monitoring. Automation in Construction vol 114. https://doi.org/10.1016/j.autcon.2020.103155

Duan J, Asteris PG, Nguyen H, Bui X-N, Moayedi H (2020) A novel artificial intelligence technique to predict the compressive strength of recycled aggregate concrete using ICA-XGBoost model. Engineering with Computers. https://doi.org/10.1007/s00366-020-01003-0

Eskandari-Naddaf H and Azimi-Pour M (2016) Performance evaluation of dry-pressed concrete curbs with variable cement grades by using Taguchi method. Ain Shams Engineering Journal. 2090-4479, https://doi.org/10.1016/j.asej.2016.09.004

Etxeberria M, Vázquez E, Marí A et al (2007) Influence of amount of recycled coarse aggregates and production process on properties of recycled aggregate concrete. Cem Concr Res 37(5):735–742. https://doi.org/10.1016/j.cemconres.2007.02.002

Evangelista L, de Brito J (2010) Durability performance of concrete made with fine recycled concrete aggregates. Cem Concr Compos 32(1):9-14.7

Fathifazl G, Razaqpur AG, Isgor OB et al (2011) Creep and drying shrinkage characteristics of concrete produced with coarse recycled concrete aggregate. Cem Concr Compos 33(10):1026–1037. https://doi.org/10.1016/j.cemconcomp.2011.08.004

González-Fonteboa B, Martínez-Abella F (2007) Shear strength of recycled concrete beams. Constr Build Mater 21(4):887–893. https://doi.org/10.1016/j.conbuildmat.2005.12.018

Hansen TC, Narud H (1983) Strength of recycled concrete made from crushed concrete coarse aggregate. Concr. Int. Des. Constr. 5(1):79–83

Hong-Guang N, Ji-Zong W (2000) Prediction of compressive strength of concrete by neural networks. Cem Concr Res 30(8):1245–1250. https://doi.org/10.1016/S0008-8846(00)003458

IS 2386:2002. Methods of Test for Aggregates for Concrete, Bureau of IndianStandards, New Delhi, India.

IS 269:2015. Ordinary Portland cement-specifications, Bureau of Indian Standards, New Delhi, India.

IS 383:2016. Coarse and fine aggregate for concrete - specification, Bureau of Indian Standards, New Delhi, India.

IS 456: 2000. Plain and reinforced concrete- code of practice, Bureau of Indian Standards, New Delhi, India.

IS 9103:1999. Concrete admixtures – specifications, Bureau of Indian Standards, New Delhi, India.

IS: 4031:2005. Method of Physical tests for hydraulic cement, Bureau of Indian Standards, New Delhi, India

IS- 516:2004. Reaffirmed, Indian Standard methods of tests for strength of concrete, Bureau of Indian Standards, New Delhi, India.

Janković K, Nikolić D, Bojović D, Lončar L, Romakov Z (2011) The estimation of compressive strength of normal and recycled aggregate concrete. Architecture and Civil Engineering 9(3):419-431 48

Lee ST (2009) Influence of recycled fine aggregates on the resistance of mortars to magnesium sulfate attack. Waste Manage 29(8):2385–2391. https://doi.org/10.1016/j.wasman.2009.04.002

Li Y, Gou J, Fan Z (2019) Particle swarm optimization-based extreme gradient boosting for concrete strength prediction. IEEE 4th Advanced Information Technology, Electronic and Automation Control Conference (IAEAC 2019). 978-1-7281-1907-6/19 ©2019 IEEE https://doi.org/10.1109/IAEAC47372.2019.8997825

Lin J, Chengwei Q, Hailang W, Junying M, Chen J, Zhang K, Li Z (2020) Prediction of cross-tension strength of self-piercing riveted joints using finite element simulation and XGBoost algorithm. Chinese Mechanical Engineering Society and Springer-Verlag Berlin Heidelberg. 34, article number 36

Liu Q, Xiao JZ, Sun ZH (2011) Experimental study on the failure mechanism of recycled concrete. Cem Concr Res 41(10):1050–1057. https://doi.org/10.1016/J.CEMCONRES.2011.06.007

Marinković S, Radonjanin V, Malešev M (2010) Comparative environmental assessment of natural and recycled aggregate concrete. Waste Manage 30(11):2255–2264. https://doi.org/10.1016/j.wasman.2010.04.012

Matias D, de Brito J, Rosa A, Pedro D (2014) "Durability of Concrete with Recycled Coarse Aggregates: Influence of Superplasticizers" Journal of materials in civil engineering volume 26 issue 7 https://doi.org/10.1061/(ASCE)MT.1943-5533.0000961

Neter, J., Kutner, M.H., Nachtsheim, C.J., Wasserman, W. (1996) Applied Linear Statistical Models. Chicago : Irwin, Fourth edition.

Newman J, Choo BS (2003) Advanced Concrete Technology Concrete Properties. Elsevier Ltd, UK

Özcan F, Atis CD, Karahan O, Uncuoğlu E, Tanyildiz H (2009) Comparison of artificial neural network and fuzzy logic models for prediction of long-term compressive strength of silica fume concrete. Adv Eng Soft 40(9):856–863. https://doi.org/10.1016/j.advengsoft.2009.01.005

Oztas A, Pala M, Ozbay E, Kanca E, Caglar N, Bhatti MA (2006) Predicting the compressive strength and slump of high strength concrete using neural network. Constr Build Mater 20(9):769–775. https://doi.org/10.1016/j.conbuildmat.2005.01.054

PedregosaScikit-learn (2011) Machine Learning in Python. Journal of Machine Learning Research 12:2825–2830

Poon CS, Chan D (2007) The use of recycled aggregate in concrete in Hong Kong. Resour Conserv Recycl 50(3):293–305. https://doi.org/10.1016/j.resconrec.2006.06.005

Poon CS, Shui ZH, Lam L (2004) Effect of microstructure of ITZ on compressive strength of concrete prepared with recycled aggregates. Constr Build Mater 18(6):461–468. https://doi.org/10.1016/j.conbuildmat.2004.03.005

Prasad D, Pandey A, Kumar B(2021) Sustainable production of recycled concrete aggregates by lime treatment and mechanical abrasion for M40 grade concrete. Construction and Building Materials. 268, https://doi.org/10.1016/j.conbuildmat.2020.121119

Purushothaman R, Ruthirapathy Amirthavalli R, Karan L (2015) Influence of Treatment Methods on the Strength and Performance Characteristics of Recycled Aggregate Concrete. J Mater Civ Eng 27(5) https://doi.org/10.1061/(ASCE)MT.1943-5533.0001128

Qian X, Wang J, Fang Y, Wang L (2018) Carbon dioxide as an admixture for better performance of OPC-based concrete. J CO2 Util 25:31–38

Ramezanianpour AA, Sobhani M, Sobhani, (2004) J. Application of a network-based neuro-fuzzy system for prediction of the strength of high strength concrete. Amirkabir J Sci Technol 15(59):78–93

Rao MC, Bhattacharyya SK, Barai SV (2011) Behaviour of recycled aggregate concrete under drop weight impact load. Constr Build Mater 25(1):69–80. https://doi.org/10.1016/j.conbuildmat.2010.06.055

RawazKurda JB, Silvestre JD (2020) A comparative study of the mechanical and life cycle assessment of high-content fly ash and recycled aggregates concrete. Journal of Building Engineering. 29. https://doi.org/10.1016/j.jobe.2020.101173

Ryu JS (2002) An experimental study on the effect of recycled aggregate on concrete properties. Mag Concr Res 54(1):7–12. https://doi.org/10.1680/macr.2002.54.1.7

Sim J, Park C (2011) Compressive strength and resistance to chloride ion penetration and carbonation of recycled aggregate concrete with varying amount of fly ash and fine recycled aggregate. Waste Manage 31(11):2352–2360. https://doi.org/10.1016/j.wasman.2011.06.014

Sivakumar N (2014) "Experimental Studies on High Strength Concrete by using Recycled Coarse Aggregate". Journal of materials in civil engineering volume 30 issue 8 https://doi.org/10.1061/(ASCE)MT.1943-5533.0002398

Soutsos MN, Tang KK, Millard SG (2011) Concrete building blocks made with recycled demolition aggregate. Constr Build Mater 25(2):726–735. https://doi.org/10.1016/j.conbuildmat.2010.07.014

Tamayo D, Silburt A, Valencia D, Menou K, Ali-Dib M, Petrovich C, Huang CX, Rein H, van Laerhoven C, Paradise A (2016) A machine learns to predict the stability of tightly packed planetary systems The American Astronomical Society. The Astrophysical Journal Letters 832:L22 (5pp). https://doi.org/10.3847/20418205/832/2/L22

Taofeek DA, Lukumon OO, Muhammad B, Anuoluwapo OA, Delgado MD, Akinade OO, Ahmed AA (2020) Deep learning in the construction industry: A review of the present status and future innovations. Journal of Building Engineering Volume (32) https://doi.org/10.1016/j.jobe.2020.101827.

Tsung Y, Yuen YC, Chao LH (2006) Properties of HPC with recycled aggregates. Cem Concr Res 36:943–950. https://doi.org/10.1016/j.cemconres.2005.11.022

Vivian WY, Wang K, Tam CM (2008) Assessing relationships among properties of demolished concrete recycled aggregate and recycled aggregate concrete using regression analysis. J Hazard Mater 152:703–714. https://doi.org/10.1016/j.jhazmat.2007.07.061

Waszczyszyn Z, Słoń ski M (2010) some problems of artificial neural networks design In: Waszczyszyn Z, editor. Advances of soft computing in engineering. CISM lectures and notes, New York, 512: . 237–316

Yilmaz I, Yuksek G (2009) Prediction of the strength and elasticity modulus of gypsum using multiple regression, ANN, and ANFIS models. Int J Rock Mech Mining Sci 46(4):803–810. https://doi.org/10.1016/j.ijrmms.2008.09.002

Yong Ho N, Pin Kelvin Lee Y, Fong Lim W, Tarek Zayed, M.ASCE (2013), "Efficient Utilization of Recycled Concrete Aggregate in Structural Concrete" Journal of materials in civil engineering volume 25 issue 3 https://doi.org/10.1061/(ASCE)MT.1943-5533.0000587

Zaharieva R, Buyle-Bodin F, Skoczylas F et al (2003) Assessment of the surface permeation properties of recycled aggregate concrete. Cem Concr Compos 25(2):223-232.8

Zhang N, Zheng LN, Duan HB, Yin F, Li J, Niu Y (2019) Differences of methods to quantify construction and demolition waste for less-developed but fast-growing countries: China as a case study. Environ Sci Pollut Res 26(25):25513–25525. https://doi.org/10.1007/s11356-019-05841-4

Zounemat-Kermani M, Stephan D, Barjenbruch M, Hinkelmann R (2020) Ensemble data mining modeling in corrosion of concrete sewer: A comparative study of network-based (MLPNN & RBFNN) and tree-based (RF, CHAID, & CART) models. Adv Eng Inform 43:101030